doi:10.6041/j.issn.1000-1298.2019.04.004

# 基于红外热成像边缘检测算法的小麦叶锈病分级研究

朱文静[1,2]　陈　华[3]　李　林[1,2]　魏新华[1,2]　毛罕平[1,2]　SPANER D[3]

(1.江苏大学现代农业装备与技术教育部重点实验室,镇江 212013;2.江苏大学农业装备工程学院,镇江 212013;
3.阿尔伯塔大学农业生命与环境科学学院,埃德蒙顿 T6G 2P5)

**摘要**:小麦叶锈病对我国小麦生产危害巨大,实现小麦叶锈病的监测和快速分级是进行科学生产管理的基础。针对常规图像检测技术的不足,提出一种基于红外热成像技术的快速检测和分级方法。首先,采集整株小麦样本的红外热成像图像,分别计算健康植株、潜伏期植株和显症植株的平均叶温,探明真菌入侵过程中的温度变化规律;然后,将经过直方图均衡化和中值滤波预处理的红外热成像中低于显症植株温度阈值的区域提取出来;通过温度区域划分、低温区域提取和阈值分割,计算病斑面积在整体植株热成像总面积中的百分比;最后,对病情指数进行相关分析,获得相关系数为 0.975 5,预测均方根误差为 9.79%,总识别正确率为 90%。结果表明,基于红外热成像边缘检测算法的小麦叶锈病分级方法是可行的。

**关键词**:小麦叶锈病;红外热成像;边缘检测;快速分级

**中图分类号**:S123　　**文献标识码**:A　　**文章编号**:1000-1298(2019)04-0036-06

# Grading of Wheat Leaf Rust Based on Edge Detection of Infrared Thermal Imaging

ZHU Wenjing[1,2]　CHEN Hua[3]　LI Lin[1,2]　WEI Xinhua[1,2]　MAO Hanping[1,2]　SPANER D[3]

(1. *Key Laboratory of Modern Agricultural Equipment and Technology*, *Ministry of Education*, *Jiangsu University*, *Zhenjiang* 212013, *China*　2. *School of Agricultural Equipment Engineering*, *Jiangsu University*, *Zhenjiang* 212013, *China*
3. *Faculty of Agricultural*, *Life and Environmental Sciences*, *University of Alberta*, *Edmonton T6G 2P5*, *Canada*)

**Abstract**: Wheat rust has a great harm to wheat production in worldwide. The rapid monitoring and classification of wheat rust is the basis for scientific production and management, and it is also the prerequisite to realize the treatment of wheat rust as soon as possible. In view of the shortcomings of conventional image detection algorithms, a fast detection and classification method based on infrared thermal imaging technology was proposed. Wheat samples were planted in a growth chamber at the University of Alberta, Canada. Growth chamber parameters settings were as following: temperature (max 15℃, min 11℃), photoperiod (day 12 h), light intensity (10 000 lx), RH (60% ~ 70%). The spring wheat variety (Peace) was susceptible to rust. The infrared thermal imager brand was FLIR E6, USA. Thermal sensitivity was less than 0.06℃; FOV was less than 45°ohorizontal × 34°overtical; IFOV was $5.2 \times 10^{-3}$ rad; IR was 160 pixels × 120 pixels. The infrared thermal imaging of the whole wheat samples were collected to calculate the average leaf temperature of the healthy plants, the submersible plants and the symptomatic plants, and the temperature changes during the invasion of the fungi were detected. Infrared thermography can be used to detect leaf temperature drop caused by pathogen infection at 6d of pathogen infection incubation period, which was 7 d ahead of the naked eye observation of leaf rust spores. The Prewitt operator (PO), Sobel operator (SO), Canny operator (CO) and Laplacian operator (LO) were used to extract the edges of visible light images. The edge extraction results of PO and SO on the lesion area was not satisfactory for the complex noise processing, and the boundary gray area was seriously ghosting. LO and CO were too lean for the edges, the detection accuracy was reduced,

收稿日期:2018-10-11　修回日期:2019-01-18

**基金项目**:国家重点研发计划项目(2017YFD0700504)、江苏省自然科学基金项目(BK20150493)、中国博士后科学基金项目(2016M601743)、江苏大学高级人才科研启动基金项目(14JDG151)和江苏高校优势学科建设工程(苏政办发〔2014〕37 号)项目

**作者简介**:朱文静(1981—),女,助理研究员,主要从事农业信息无损检测研究,E-mail:zwj0410@foxmail.com

**通信作者**:魏新华(1972—),男,研究员,博士生导师,主要从事农业信息化及智能化农业装备研究,E-mail:wxh@ujs.edu.cn

and the background error was too large. Obviously, the direct use of conventional edge detection operators cannot meet the ultimate goal of rapid classification of diseases. Therefore, a fast detection and classification method based on infrared thermal imaging technology was proposed. The experiment was divided into two kinds of extraction methods: single leaf and whole plant. When the whole plant was extracted, the flower pot was removed and only the wheat plant was kept for extraction. From the results of the whole wheat extraction, the area of the whole plant disease can be extracted successfully by the method of area occupation ratio calculation based on the temperature edge. The error of the regional extraction results of the single leaf focus was slightly larger than that of the single leaf focus, but the final calculation results were satisfactory. The region below the temperature threshold was extracted from the infrared thermal image which was preprocessed by histogram equalization and median filtering. The ratio of lesion area to total area of plant thermography was calculated after three steps, including temperature division, low temperature region extraction and threshold segmentation. Finally, the correlation analysis was carried out with the disease index. The correlation coefficient was 0.975 5, the root mean square error was 9.79%, and the overall recognition rate was 90%. The research result showed that the wheat leaf rust classification method based on the infrared thermal imaging temperature information was feasible. It provided the theoretical and method basis for the early scientific application and the establishment of more accurate disease identification expert system.

**Key words**: wheat leaf rust; infrared thermal imaging; edge detection; rapid classification

## 0　引言

小麦叶锈病是由小麦隐匿柄锈菌(*Puccinia triticina*)引起的一种世界性重要病害,严重时可造成40%以上的产量损失。近年来全球气候变暖以及耕作制度改变更促使小麦叶锈病的发生和蔓延[1]。病害高发、过量施药,从而导致作物产量和质量严重下降、农田污染严重。因此,实时、灵敏、可靠的小麦病害监测和预警对小麦科学生产管理具有重要意义。

红外热成像技术以其对温度的高敏感性和可在线检测特点,目前在电气[2]、航空[3]、植保[4]、育种[5]和医学[6]等领域均有比较成熟的研究成果[7],在农业生产的诸多领域也有相关的应用[8-9]。在植物病害的检测方面有较多研究[10-21]。目前基于红外热成像技术的图像处理研究基本围绕温度的测量和分析展开,无论是生物或非生物胁迫,主要评价指标为叶片和植株平均温度(Average temperature, AT)、叶片的最大温差(Maximum temperature difference, MTD)等[22]。

边缘检测是数字图像处理的重要内容,是解析作物图像的前提。其基本原理是利用图像在边缘处的阶跃性,按照某种方法检测出边缘点并将其连接构成分割区域,从而实现目标与背景的分离。已有研究者将边缘检测用于红外热像的分析研究。RAZA 等[23]采用静态小波变换成功提取病害植物的热像图和可见光图轮廓并进行配准。JIAO 等[24]研究了桃子表面腐烂的监测方法和腐烂部分边缘的提取和计算方法。王栋等[25]提出一种改进的蚁群算法,能够在热像图边缘丰富区域搜索的同时抑制算法结果早熟,缩短运行时间。陈浩等[26]将蚁群算法引入到玉米干旱的热成像图处理中,并提出将边缘检测用于红外热像分析中。李存兵等[27]提出基于小波变换的水果边缘检测方法,识别结果优于拉普拉斯等其他算法。周建民等[28]利用高低帽算子结合基于直方图的全局阈值分割红外热像图,识别树上板栗的空心果和坏死果。目前利用红外热成像的边缘检测处理开展作物病害分级的研究较少。

本文以感染叶锈病的小麦叶片为研究对象,基于红外热成像边缘检测算法提取病斑的具体区域,根据病斑面积占比确定染病程度和病害等级,最后对病情指数结果进行相关分析和叶锈病分级。

## 1　材料与方法

### 1.1　样本培育与病毒接种

小麦样本培育在加拿大阿尔伯塔大学北校区农业生命与环境科学学院智能人工气候生长室进行,如图1a所示。最高温度15℃,最低温度11℃;每天光照时间12 h;光照强度10 000 lx,相对湿度60%~70%。选用加拿大易感病小麦品种Peace,硬粒,其籽粒外皮为红色,蛋白质含量在14%左右。硬粒小麦品质好,籽粒蛋白质含量高,同样也是我国普遍种植的小麦品种,且我国小麦蛋白质含量平均为15%左右,与Peace非常接近。从叶锈病的病原菌看,我国与加拿大的叶锈病均由小麦隐匿柄锈菌菌种感染,都是通过孢子萌发时产生若干个小孢子,侵染转主寄主,产生锈子器和性子器。基于以上分析可知加拿大Peace小麦品种与我国易感病小麦品种相似,而小麦

叶锈病在我国是极为多发的小麦真菌病害,从两国叶锈病的菌种、传播途径和侵染方式上看都具有一致性,因此选用该品种进行试验。因此本文方法在检测国内感染叶锈病的小麦时也可以使用。

待小麦生长至两片真叶时进行喷雾接种,如图 1b 所示。接种步骤为:①用蒸馏水淋湿生长室内壁,将小麦在湿度较大的空间放置 30 ~ 45 min。②配置真菌孢子喷雾液,先从超低温冰箱取出橙红色粉状孢子,放置 45℃水浴锅中 5 min 发生热休克反应,然后用吐温 20 配置成悬浮液,质量浓度为 3 g/mL。③在通风橱内进行喷雾接种,通风橱在喷雾前和使用后均用 70% 乙醇消毒,喷雾器用 70% 酒精彻底清洗后用蒸馏水洗净,从上至下进行喷雾,直至麦苗有水滴状液滴落下即可。④每盆小麦在喷雾后使用一个透明高压蒸汽袋覆盖,如图 1c 所示。⑤高压蒸汽袋覆盖 24 h 后取下,将小麦放回到生长室。

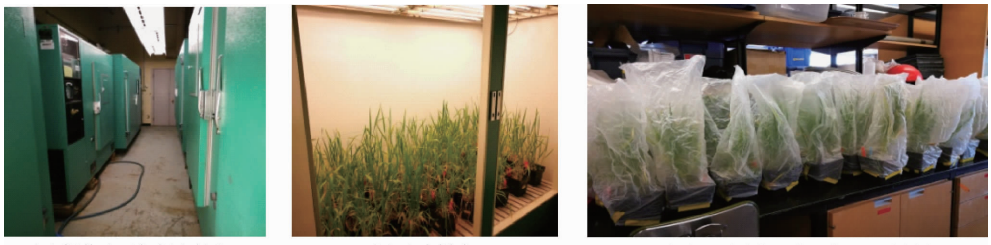

(a) 智能人工气候生长室 (b) 小麦样本 (c) 接种后覆盖高压蒸汽袋的小麦样本

图 1 样本培育和喷雾接种现场

Fig. 1 Sample cultivation and spray inoculation scene

### 1.2 试验仪器与图像采集

试验仪器为美国菲力尔公司 FLIR E6 型热成像仪。该热成像仪可同时拍摄可见光图像和红外热成像图像;温度热灵敏测量精度为 0.06℃;测温范围为 -20 ~ 250℃;拍摄模式为中央点偏重测光模式;视场角为水平 45° × 垂直 34°;瞬时视场 $5.2 \times 10^{-3}$ rad;红外图像分辨率为 160 像素 × 120 像素。

红外热像图采集期间,室温保持在 20℃,相对湿度 50%,采集背景保持一致。拍摄时按照样本编号顺序取出,拍摄后立即放回生长室,以保障每个样本的拍摄一致性。

### 1.3 病情指数获取

接种 12 d 后叶面开始出现孢子堆,接种 21 d 后病害进入盛发期。根据我国小麦叶锈病测报调查规范(NY/T 617—2002),严重度指病叶上叶锈菌夏孢子堆所占面积与叶片总面积的百分比,用分级法表示,分为 1%、5%、10%、20%、40%、60%、80% 和 100% 8 个级别(Grade,G)。每个级别选取 10 个叶片作为重复。小麦样本生长周期为拔节期向抽穗期过渡;每个样本拍摄完红外热成像图像后同时记录下人工调查法获得的病害等级。具体方法:每株小麦调查倒三叶、倒二叶、旗叶 3 片叶片,每盆 8 株小麦,共计 24 片叶片。反映发病程度的普遍率 $I$、平均严重度 $S$、病情指数(Disease index,DI)的计算公式为

$$I = \frac{n}{N} \times 100\% \tag{1}$$

$$S = \frac{\sum_{i=1}^{8} (s_i n_i)}{n} \tag{2}$$

$$D_I = IS \tag{3}$$

式中 $n$——发病叶片数

$N$——每盆小麦叶片总数

$s_i$——$i$ 级严重度,%

$n_i$——$i$ 级严重度的病叶数

$D_I$——病情指数,%

### 1.4 红外热成像图预处理

整盆小麦植株样本的红外热成像图如图 2a 所示。对红外热成像图进行直方图均衡化处理。彩色图像的直方图均衡化主要是将各个像素归一化后的灰度值赋给该像素,对图像的色彩、亮度等信息进行修正,使修正后的图像更加生动、色彩更加鲜艳,细节更加突出,如图 2b 所示。中值滤波法是一种非线性平滑技术,它将每一像素点的灰度设置为该点某

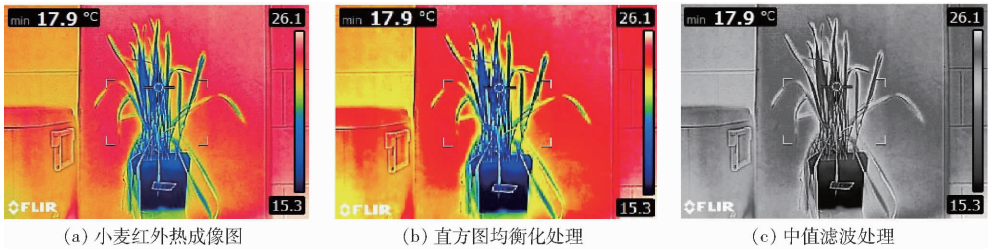


(a) 小麦红外热成像图 (b) 直方图均衡化处理 (c) 中值滤波处理

图 2 小麦红外热成像图及预处理后的图像

Fig. 2 Infrared thermal imaging and processed image of wheat

邻域窗口内所有像素点灰度的中值，是在“最小绝对误差”准则下的最优滤波，中值滤波处理后的图像如图 2c 所示。

对小麦叶锈病的红外热成像图的分析和处理是基于 FLIR 软件和 Matlab R2010a 软件平台。

## 2　结果与分析

### 2.1　红外热成像图随病害发展的温度动态分析

平均叶温的测定方法：每盆小麦样本固定一个叶片为检测对象，从接种第 1 天到接种后 12 d，每天拍摄该叶片的红外热成像图，并用 FLIR 软件提取叶片区域的平均温度。图 3 显示了健康组、潜伏期组和发病组样本的平均温度变化趋势，结果显示健康组小麦植株的平均温度在整个检测期内的波动范围为 19.5 ~ 19.8℃，而发病组小麦植株平均温度为 18.3 ~ 18.7℃。潜伏期组小麦植株平均温度呈现逐步下降的趋势，从第 1 天的 19.9℃降至第 12 天的 18.8℃。通过连续的温度监测，表明接种后第 6 天染病叶片的温度较正常叶片下降达 0.4℃，随后温差逐渐增大，能够将接种病菌的小麦植株和健康小麦植株区分开，比人工调查法提前了 7 d 检测到病菌感染。一方面表明红外热成像能够在显症之前就检测到病菌的感染，及早施药可减少用药量；另一方面，在后续的边缘检测算法中，选用潜伏期组的红外热成像图有助于早期诊断。

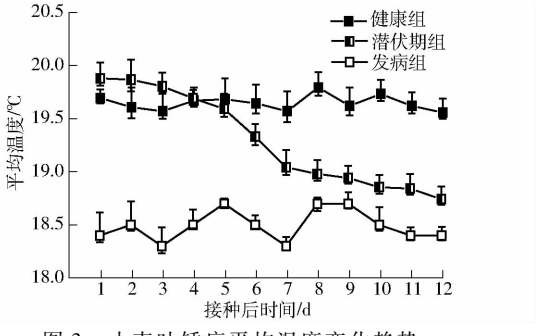


图 3　小麦叶锈病平均温度变化趋势

Fig. 3　Changing trend of average leaf temperature in wheat leaf rust

### 2.2　病斑区域常规算法边缘提取

边缘检测算法是图像处理和计算机视觉中，尤其是特征提取中的一个重要研究方法。然而在可见光图像中，自然界图像的边缘并不总是理想的阶梯边缘。相反，可见光图像通常受到诸多因素的影响，例如有限场景深度带来的聚焦模糊，光滑物体边缘的阴影，以及物体边缘附近的局部镜面反射或漫反射等。图 4a 为红外热像仪采集到的小麦叶片可见光图像，分别采用较为常用的一阶导数中的最大值和最小值来检测边界的 Prewitt 算子（PO）、Sobel 算子（SO）和通过寻找图像二阶导数过零点来检测边界的 Canny 算子（CO）、Laplacian 算子（LO）对可见光图像进行边缘提取，提取结果如图 4b ~ 4e 所示。

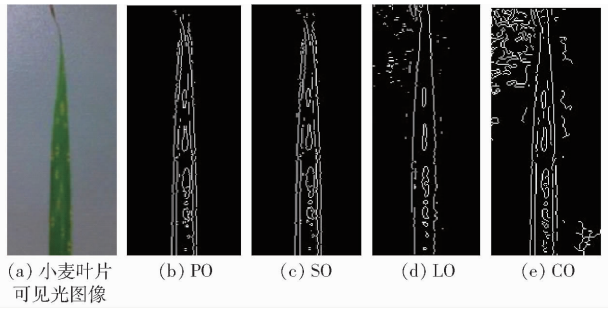


图 4　4 种常规边缘检测算子的小麦叶锈病单叶识别结果

Fig. 4　Four kinds of commonly used edge detection operators for single leaf identification of wheat leaf rust

从图 4b ~ 4e 可以看出，PO 和 SO 对病斑区域的边缘提取结果存在对混合复杂噪声处理效果不理想的问题，边界灰度区域重影严重。而 LO 和 CO 由于太追求过细的边缘，检测精度降低，背景误测也较大。这是由于小麦锈病的发病区域不集中，而是星星点点，呈现十多处小区域，这些区域即发病严重之后产生孢子堆的位置，要将这十多个区域都提取出来，显然直接运用常规的边缘检测算子不能实现病害快速分级。

### 2.3　基于红外热成像边缘检测算法的病斑面积提取

相对于直接使用常规边缘检测算子，本研究通过提取红外热成像图的温度信息，对温度信息的边界进行划分，计算病斑面积与叶片面积百分比来对小麦叶锈病进行分级。

图 5 为基于红外热成像边缘检测算法的病害面积提取步骤。图 5a 为红外热成像原图，随着叶锈病真菌的不断侵入，病菌经微伤口进入临近的活体细胞繁殖，导致蒸腾作用加剧，从而使感病部位水分大量散失，局部温度下降。由 2.1 节的分析可知，叶片平均温度在潜伏期内会随着真菌繁殖的加剧从 20℃左右下降至 18.5℃左右。因此以 18.5℃为临界值对温度实施阈值划分，如图 5b 所示。通过温度阈值划分，将叶片内低于 18.5℃的温度边缘提取出来，用蓝色显示，如图 5c 所示。采用最大类间方差法寻找最合适的阈值，该方法计算出的阈值通常比人为设定的阈值能更好地把灰度图像转换为二值图像，如图 5d 所示。进一步对图像进行分割，计算出叶片总面积和病斑区域面积，分别如图 5e 和图 5f 所示。病斑区域面积与叶片总面积的百分比即为病害的占比指数。

从整体检测结果看，基于红外热成像边缘检测算法的病斑面积百分比，可实现叶锈病的等级识别。

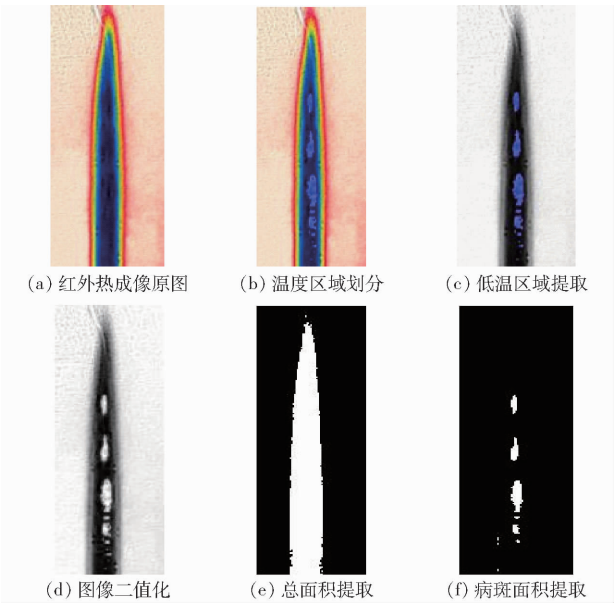


图 5 基于红外热成像边缘检测算法的病害面积提取步骤

Fig. 5 Extraction procedure of lesion area based on temperature edge

然而单叶检测在实际生产中意义不大,为实现整株小麦快速在线检测的要求,进一步对整株染病小麦的热成像图进行分析。整株小麦病害面积提取结果如图 6 所示。

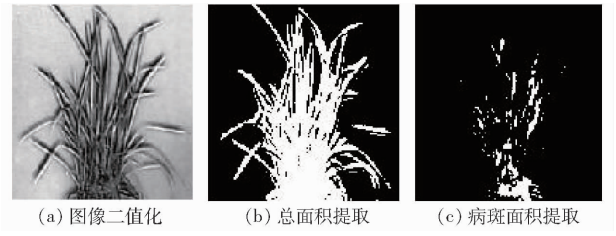


图 6 基于红外热成像边缘检测算法的整株小麦病害面积提取

Fig. 6 Area extraction of whole plant disease based on temperature edge detection algorithm

去除花盆部分,仅保留小麦植株部分,从整株小麦的提取结果看,对红外热成像原图进行温度区域划分和低温区域提取后,再经过图像二值化、整株面积提取和病斑面积提取后,基于红外热成像边缘检测算法的病斑面积百分比可以成功提取整株小麦的病害区域,比单叶病斑区域的提取结果误差略大,但提取效果和最终计算结果较优。本文通过 Photoshop 获取实际病斑位置,并与基于红外热成像边缘检测算法得到的病斑位置进行比较,两者结果基本一致,说明该方法的分割性能良好。

## 2.4 分级识别结果与分析

利用本文算法对 40 株小麦植株样本进行处理,得到病斑面积百分比的预测值,并归入病害严重度相应级别。将 40 株小麦的病斑面积百分比预测值与其病情指数 $D_I$ 作相关性分析,结果如图 7 所示,得到相关系数 $R$ 为 0.975 5,预测均方根误差为 9.79%。

表 1 为 40 株小麦叶锈病整株识别样本的病情

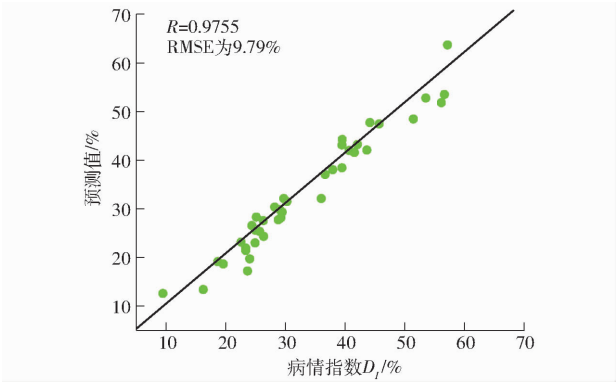


图 7 小麦样本病情指数与预测值的相关性分析

Fig. 7 Correlation analysis of predicted value and disease index of wheat samples

**表 1 基于红外热成像边缘检测算法的小麦叶锈病病情指数预测值和定级结果**

**Tab. 1 Prediction and grading results of $D_I$ based on infrared thermal imaging edge detection of wheat leaf rust** %

| 样本 | 病情指数(级别) | 病情指数预测值(级别) |
|---|---|---|
| 1 | 24.48(4) | 26.60(4) |
| 2 | 16.32(3) | 13.42(3) |
| 3 | 22.66(4) | 23.20(4) |
| 4 | 25.11(4) | 25.61(4) |
| 5 | 28.29(4) | 30.40(4) |
| 6 | 23.44(4) | 21.45(4) |
| 7 | 25.78(4) | 25.39(4) |
| 8 | 19.67(3) | 18.69(3) |
| 9 | 23.75(4) | 17.25(3) |
| 10 | 29.81(3) | 32.18(3) |
| 11 | 25.01(4) | 23.03(4) |
| 12 | 25.21(4) | 28.35(4) |
| 13 | 29.55(4) | 29.38(4) |
| 14 | 28.91(4) | 27.80(4) |
| 15 | 29.17(4) | 29.86(4) |
| 16 | 24.11(4) | 19.74(3) |
| 17 | 29.35(4) | 28.18(4) |
| 18 | 38.02(4) | 38.09(4) |
| 19 | 42.19(5) | 43.28(5) |
| 20 | 44.27(5) | 47.79(5) |
| 21 | 40.76(5) | 42.08(5) |
| 22 | 56.77(5) | 53.58(5) |
| 23 | 56.25(5) | 51.89(5) |
| 24 | 41.67(5) | 41.63(5) |
| 25 | 39.63(4) | 44.31(4) |
| 26 | 51.56(5) | 48.53(5) |
| 27 | 36.76(4) | 37.12(4) |
| 28 | 39.58(4) | 43.19(4) |
| 29 | 45.83(4) | 47.51(4) |
| 30 | 36.11(4) | 32.16(4) |
| 31 | 53.65(4) | 52.86(4) |
| 32 | 43.75(4) | 42.14(4) |
| 33 | 57.29(4) | 63.78(5) |
| 34 | 26.39(4) | 27.61(4) |
| 35 | 26.45(4) | 24.37(4) |
| 36 | 30.36(4) | 31.54(4) |
| 37 | 23.44(4) | 21.97(4) |
| 38 | 39.58(4) | 38.49(4) |
| 39 | 18.75(3) | 19.17(3) |
| 40 | 9.55(2) | 12.61(3) |

指数预测结果。从表中可以看出，样本 9、16、33 和 40 的整株识别的定级有误。样本 9 和 16 将 4 级误判为 3 级，样本 33 将 4 级误判为 5 级，样本 40 将 2 级误判为 3 级，其余 36 个样本均评级正确，总识别正确率达到 90%。

## 3　结论

（1）红外热成像技术能够在病原菌侵染的第 6 天检测到病菌感染，比人工调查法提前 7 d 检测到叶锈病真菌感染。

（2）对 40 株小麦叶锈病样本的病斑面积百分比预测值和病情指数 $D_I$ 作相关性分析，得到相关系数 $R$ 为 0.975 5，预测均方根误差为 9.79%。40 个样本中有 4 个样本定级错误，36 个样本定级正确，总识别正确率为 90%，说明运用本文算法对小麦叶锈病进行诊断是可行的。

## 参　考　文　献


[1] 金夏红，冯国华，刘东涛，等. 小麦抗叶锈病遗传研究进展[J]. 麦类作物学报，2017，37(4)：504－512.
JIN Xiahong, FENG Guohua, LIU Dongtao, et al. Review on genetic research on leaf rust in wheat[J]. Journal of Triticeae Crops, 2017, 37(4): 504－512. (in Chinese)

[2] 李真，史智兴，王成，等. 红外热成像技术在作物胁迫检测方面的应用[J]. 农机化研究，2016，38(1)：232－237.
LI Zhen, SHI Zhixing, WANG Cheng, et al. The application progress of infrared thermography for crop stress detection[J]. Journal of Agricultural Mechanization Research, 2016, 38(1): 232－237. (in Chinese)

[3] GUO Jiuxin, TIAN Guangli, ZHOU Yi. Evaluation of the grain yield and nitrogen nutrient status of wheat (*Triticum aestivum* L.) using thermal imaging[J]. Journal of Animal & Plant Sciences, 2015, 25(3): 202－207.

[4] JIAO Leizi , DONG Daming, FENG Haikuan, et al. Monitoring spray drift in aerial spray application based on infrared thermal imaging technology[J]. Computers & Electronics in Agriculture, 2016, 121(C): 135－140.

[5] FANG Wenhui, LU Wei, XU Hongli, et al. Study on the detection of rice seed germination rate based on infrared thermal imaging technology combined with generalized regression neural network[J]. Spectroscopy & Spectral Analysis, 2016, 36(8): 2692－2697.

[6] JIAN Bolin, CHEN Chiehli, CHU Wenlin, et al. The facial expression of schizophrenic patients applied with infrared thermal facial image sequence[J]. BMC Psychiatry, 2017, 17(1): 229－236.

[7] 陈斌，田桂华. 红外热成像技术在植物病害检测中的应用研究进展[J]. 江苏农业科学，2014，42(9)：1－4.
CHEN Bin, TIAN Guihua. Research progress of application of infrared thermography in plant disease detection[J]. Jiangsu Agricultural Sciences, 2014, 42(9): 1－4. (in Chinese)

[8] 周建民，周其显，刘燕德. 红外热成像技术在农业生产中的应用[J]. 农机化研究，2010，32(2)：1－4.
ZHOU Jianmin, ZHOU Qixian, LIU Yande. Application of infrared thermography techniques in agricultural production[J]. Journal of Agricultural Mechanization Research, 2010, 32(2): 1－4. (in Chinese)

[9] JIAO Litao, WU Weibing, ZHENG Wanguo, et al. The infrared thermal image-based monitoring process of peach decay under under uncontrolled temperature conditions[J]. Journal of Animal and Plant Sciences, 2015, 25(1): 202－207.

[10] MASRI A A, HAU B, DEHNEH W, et al. Impact of primary infection site of Fusarium species on head blight development in wheat ears evaluated by IR-thermography[J]. European Journal of Plant Pathology, 2016, 147(4): 1－14.

[11] ANKUSH P, HSMLYN G J. Assessing drought responsesusing thermal infrared imaging[J]. Environmental Responses in Plants, 2016, 1398 (6): 209－219.

[12] CHEN Zilong, REN Xiangrong, CONG Hua, et al. Study on the relationship between the winter wheat thermal infrared image characteristics and physiological indicators[J]. International Symposium on Optoelectronic Technology and Application: Infrared Technology and Applications, 2014, 11: 291－298.

[13] ALIREZA E, KAZEM P, HOJAT A, et al. Use of IR thermography in screening wheat (*Triticum aestivum* L.) cultivars for salt tolerance[J]. Archives of Agronomy & Soil Science, 2016, 63(2): 161－170.

[14] MAHLEIN A K, OERKE E C, STEINER U, et al. Recent advances in sensing plant diseases for precision crop protection[J]. European Journal of Plant Pathology, 2012, 133(1): 197－209.

[15] ZHANG Yan, MENG Qinglong, SHANG Jing, et al. The application and perspective of new imaging technology in detection of plant diseases[J]. Laser Journal, 2017, 38(12): 7－13.

[16] 李小龙，王库，马占鸿，等. 基于热红外成像技术的小麦病害早期检测[J]. 农业工程学报，2014，30(18)：183－189.
LI Xiaolong, WANG Ku, MA Zhanhong, et al. Early detection of wheat disease based on thermal infrared imaging[J]. Transactions of the CSAE, 2014, 30(18): 183－189. (in Chinese)

[17] OERKE E C, FROHLING P, STEINER U. Thermographic assessment of scab disease on apple leaves[J]. Precision Agriculture, 2011, 12(5): 699－715.

[18] BELIN É, ROUSSEAU D, BOUREAU T, et al. Thermography versus chlorophyll fluorescence imaging for detection and quantification of apple scab[J]. Computers and Electronics in Agriculture, 2013, 90: 159－163.

[19] WANG Fei, OMASA K, XING Shangjun, et al. Thermographic analysis of leaf water and energy information of Japanese spindle and glossy privet trees in low temperature environment[J]. Ecological Informatics, 2013, 16: 35－40.

[20] WANG Min, LING Ning, DONG Xian, et al. Thermographic visualization of leaf response in cucumber plants infected with the soilborne pathogen *Fusarium oxysporum* f. sp. *cucumerinum*[J]. Plant Physiology and Biochemistry, 2012, 61: 153－161.


（下转第 48 页）

QI Long, JIANG Yu, LI Zehua, et al. Automatic detection and counting method for spores of rice blast based on micro image processing [J]. Transactions of the CASE, 2015, 31(12):186 - 193. (in Chinese)

[16] 姜玉英, 罗金燕, 罗德平,等. 远程控制病菌孢子捕捉仪对小麦气传病害的监测效果[J]. 植物保护, 2015,41(6):163 - 168.
JIANG Yuying, LUO Jinyan, LUO Deping, et al. Monitoring effect of remote-controlled spore trap on wheat aero-borne diseases [J]. Plant Protection, 2015,41(6):163 - 168. (in Chinese)

[17] 雷雨,姚志凤,何东健. 小麦条锈病菌夏孢子显微图像远程采集系统设计与试验[J/OL]. 农业机械学报,2018,49(11):39 - 47.
LEI Yu, YAO Zhifeng, HE Dongjian. Design and experiment of micro-image remote acquisition system of uredinispores of *Puccinia striiformis* f. sp. *tritici* [J/OL]. Transactions of the Chinese Society for Agricultural Machinery, 2018, 49(11): 39 - 47. http://www.j-csam.org/jcsam/ch/reader/view_abstract.aspx? file_no = 20181105&flag = 1&journal_id = jcsam. DOI: 10.6041/j.issn.1000-1298.2018.11.005. (in Chinese)

[18] MELO C, LOPES J G, ANDRADE A O, et al. Semi-automated counting of arbuscular mycorrhizal fungi spores using artificial neural network [J]. IEEE Latin America Transactions, 2017, 15(8):1566 - 1573.

[19] ROY M, JIN G, SEO D. A simple and low-cost device performing blood cell counting based on lens-free shadow imaging technique [J]. Sensors & Actuators B Chemical, 2014, 201(4):715 - 723.

[20] SEO D, ROY M, KIM J. High-throughput and real-time microalgae monitoring platform using lens-free shadow imaging system (LSIS) [C]// Sensors, IEEE,2016:1 - 3.

[21] ZHANG X, KHIMJI I, GURKAN U A. Lensless imaging for simultanrous microfluidic sperm monitoring and sorting [J]. Lab on a Chip, 2011, 11(15):2535 - 2540.

[22] LI G X, ZHANG R B, YANG N, et al. An approach for cell viability online detection based on the characteristics of lensfree cell diffraction fingerprint [J]. Biosensors and Bioelectronics,2018,107:163 - 169.

[23] THOMAS B P, RAJENDREN K V, PILLAI S A. Wholefield NDT of porous materials using digital holography[C]// Proc. National Seminar on Non-Destructive Evaluation. Hyderabad: Indian Society for Non-Destructive Testing, 2006:229 - 234.

[24] LEE Y H, KASSAM S A. Generalized median filtering and related nonlinear filtering techniques [J]. Acoustics Speech & Signal Processing IEEE Transactions on, 1985, 33(3):672 - 683.

[25] MUDANYALI O, TSENG D, OH C. Compact, Light-weight and cost-effective microscope based on lensless incoherent holography for telemedicine applications [J]. Lab on a Chip, 2010, 10(11):321 - 328.

[26] 许燎原, 赵丽稳, 胡宇峰,等. 稻瘟病菌孢子 qPCR 方法的建立及用于监测气传菌源的研究[J]. 浙江农业学报, 2016, 28(8):1368 - 1373.
XU Liaoyuan, ZHAO Liwen, HU Yufeng, et al. Development of a qPCR detection method for monitoring conidial density of rice blast fungus in the air [J]. Acta Agriculturae Zhejiangensis,2016,28(8):1368 - 1373. (in Chinese)

[27] 陈浩,康晓慧,张梅,等. 稻瘟病菌空中孢子量与气象因子的关系[J]. 湖北农业科学,2009,48(8):1869 - 1871.
CHEN Hao, KANG Xiaohui, ZHANG Mei, et al. Relationship between spatial spore amount of *Pyricularia oryzae* cavara and meteorological factors [J]. Hubei Agricultural Science, 2009,48(8):1869 - 1871. (in Chinese)

(上接第 41 页)

[21] 徐小龙,蒋焕煜,杭月兰. 热红外成像用于番茄花叶病早期检测的研究[J]. 农业工程学报,2012, 28(5): 145 - 149.
XU Xiaolong, JIANG Huanyu, HANG Yuelan. Study on detection of tomato mosaic disease at early stage based on infrared thermal imaging[J]. Transactions of the CSAE, 2012, 28(5): 145 - 149. (in Chinese)

[22] MAHLEIN A K, OERK E C, STEINER U, et al. Recent advances in sensing plant diseases for precision crop protection[J]. European Journal of Plant Pathology, 2012, 133(1): 197 - 209.

[23] RAZA S A, SANCHEZ V, PRINCE G, et al. Registration of thermal and visible light images of diseased plants using silhouette extraction in the wavelet domain[J]. Pattern Recognition, 2015,48(7): 2119 - 2128.

[24] JIAO Leizi, WU Weibing, ZHENG Wenge, et al. The infrared thermal image-based monitoring process of peach decay under uncontrolled temperature conditions[J]. Journal of Animal and Plant Sciences, 2015, 25(3Supp. 1): 202 - 207.

[25] 王栋,尚堃. 基于改进蚁群算法的红外图像边缘检测方法[J]. 四川兵工学报, 2014, 35(7): 87 - 90.
WANG Dong, SHANG Kun. Edge detection algorithm of image based on improved ant colony optimization[J]. Journal of Sichuan Ordnance, 2014, 35(7): 87 - 90. (in Chinese)

[26] 陈浩,方勇,朱大洲,等. 基于蚁群算法的玉米植株热红外图像边缘检测[J]. 农机化研究,2015,37(6): 49 - 52.
CHEN Hao, FANG Yong, ZHU Dazhou, et al. Thermal infrared image edge detection method based on ant colony algorithm for corm plant[J]. Journal of Agricultural Mechanization Research, 2015, 37(6): 49 - 52. (in Chinese)

[27] 李存兵,姜伟,华金. 基于小波变换的水果红外图像目标识别[J]. 机电工程,2007,24(8): 24 - 26.
LI Cunbing, JIANG Wei, HUA Jin. Wavelet transformation for infared fruit images object identify[J]. Mechanical and Electrical Engineering, 2007, 24(8): 24 - 26. (in Chinese)

[28] 周建民,尹洪妍,张瑞丰,等. 基于红外热成像树上板栗机器识别研究[J]. 中国农机化学报,2012,33(3): 132 - 136.
ZHOU Jianmin, YIN Hongyan, ZHANG Ruifeng, et al. Study on machine recognition of Chinese chestnut on trees based on infrared thermograghy[J]. Chinese Agricltural Mechanization, 2012, 33(3): 132 - 136. (in Chinese)